Monte Carlo simulations of electron interactions with the DNA molecule: A complete set of physics models for Geant4-DNA simulation toolkit

Sara A. Zein[1*], Marie-Claude Bordage[2*], Hoang Ngoc Tran[1], Giovanni Macetti[3], Alessandro Genoni[3], Claude Dal Cappello[3], Sébastien Incerti[1]

[1]Univ. Bordeaux, CNRS, LP2I Bordeaux, UMR 5797, F-33170 Gradignan, France
[2] Université Paul Sabatier, UMR1037 CRCT, INSERM, F-31037 Toulouse, France
[3] Université de Lorraine & CNRS, Laboratoire LPCT (UMR 7019), 1 Boulevard Arago, 57078 Metz, France

[*]Both authors contributed equally

Corresponding Author:
Sara A. Zein
Laboratoire de Physique de Deux Infinis de Bordeaux
19 chemin du Solarium
33175 Gradignan, France
Telephone: +33 5 57 12 08 89
Email: zein@lp2ib.in2p3.fr

Email addresses
zein@lp2ib.in2p3.fr
marie-claude.bordage@inserm.fr
tran@lp2ib.in2p3.fr
giovanni.macetti@univ-lorraine.fr
alessandro.Genoni@univ-lorraine.fr
claude.dal-cappello@univ-lorraine.fr
incerti@lp2ib.in2p3.fr

Abstract

In this study we are introducing an update of the Geant4-DNA physics constructor “option 6” including electron interactions with all constituents of the DNA molecule in addition to those already publicly available for liquid water. The new implementation is based on the interaction cross sections of electrons with the four DNA nucleobases, deoxyribose and phosphoric acid for elastic scattering, electronic excitation and ionisation in the 11 eV – 1 MeV energy range. An additional sampling method to estimate the transferred secondary electron energy produced by ionisation is also introduced and can be optionally activated instead of the classical interpolation method based on the differential cross section tables, thus eliminating the need to upload large data files. The implementation in Geant4-DNA was verified by calculating range and electronic stopping power in the various materials. Good agreement is observed with the data available in the literature, and calculations with the interpolation method and the sampling method showed less than 4% difference. No differences were observed in terms of computational cost.

Keywords: Geant4-DNA, DNA material, Monte Carlo, Electron cross sections, sampling method, Stopping power, Range.

Highlights:

- Electron interactions in DNA material
- Geant4-DNA electron transport in DNA
- Electron stopping power in DNA
- Electron range in DNA
- Ionisation sampling method

I. Introduction:

In studies of radiotherapy and radiobiology, radio-induced damage to the DNA molecule is of upmost interest since it directly affects the mortality of cells and the integrity of their replication, function and genetic expression [1]. Therefore, DNA is considered the most radio-sensitive target of the cell and radiation interaction with the backbone of the DNA (with deoxyribose sugar and phosphate group as its main components) is essential to estimate the DNA fragmentation, mostly identified by DNA strand breaks that are damages difficult to repair. In addition, damages and alterations of the nucleobases result in mutations and irregular gene expressions [2]. Upon impact, ionising radiation induces DNA damages by physical effects, through the direct ionisation and excitation of the molecule itself or, indirectly, through the creation of reactive oxygen species in the cellular medium that attack the DNA molecule. In radiobiology applications, medical physics and radioprotection, Monte Carlo simulations have been used to estimate such effects and considerable efforts have been made in the development of track structure codes able to model the radiation interaction with biological material, particularly the most abundant liquid water [3]. These codes include PARTRAC, KURBUC, CPA100 and Geant4-DNA [4]. PARTRAC provides options for simulating the different radiation interaction stages in water targets, such as DNA damage and repair [5]. KURBUC [4] and CPA100 [6] simulate the physical and chemical stages of electron interaction in water and CPA100 can additionally track electrons in DNA material [7, 8]. The Geant4-DNA simulation toolkit [9-12], the low-energy physics extension of the open source Geant4 toolkit [13-15], tracks electrons during the physical stage in liquid water as well as in the chemical stage up to 1μs after the first impact to model water radiolysis [16].

Track structure codes consider that the biological medium mainly consists of water since water constitutes up to 70% of living beings. Therefore, simulation studies on DNA damage available in the literature estimate the damages from particle-water interaction [5, 17, 18]. In addition, considering the medium homogeneously filled with liquid water simplifies the calculations and gives a good assumption for an overall dose estimation. However, for DNA damage calculation, this may not be very accurate since the DNA density is higher than water [19] and the probability for particle-DNA interaction is also higher as shown by particle-DNA interaction cross section values [20]. This limitation motivates the need for more accurate particle-DNA interaction simulations.

A recent work by Zein *et al.* [20] introduced a new development of the Geant4-DNA toolkit to extend the “option 6” physics constructor to electrons in DNA nucleobases. This constructor, which is publicly available for liquid water in the 11 eV – 256 keV energy range

[21], is based on the CPA100 Fortran-code written by Terrissol *et al.* [6] for electron interactions. CPA100 not only tracks electrons in water but also in DNA constituents: the nucleobases adenine, thymine, guanine and cytosine as well as deoxyribose sugar and the phosphate group [22]. In the recent extension of the "option 6" physics models, interaction cross-sections of electrons with the four nucleobases were calculated for elastic scattering, electronic excitation, and ionisation over the 11 eV - 1 MeV energy range, where they showed good agreement with experiments and calculations reported in the literature. Electronic stopping power, continuous slowing down approximation (CSDA) range and inelastic mean free path were calculated using the cross-sections' implementation in Geant4-DNA [20].

In this study, we are complementing this previously published work by calculating the electron cross-sections over the 11 eV - 1 MeV energy range in the deoxyribose and phosphoric acid (bound state of the phosphate group), which constitute the backbone of the DNA molecule. This allowed us to provide a complete set of electron interaction cross-sections for DNA in addition to those previously available for liquid water. While extending the "option 6" constructor, we noticed that the excitation interaction for the four nucleobases was not being adequately sampled and upon testing we noticed that the electron ranges were affected for very low energies only. Therefore, after fixing the bug in the code, we have recalculated the CSDA range of electrons in the four nucleobases and we are presenting the corrected results in this work in addition to the newly introduced values in deoxyribose and phosphoric acid. It is also worth noting that, with the increasing number of materials, the size of the cross-section tables become large, especially regarding the differential cross sections for ionisation. Furthermore, since the number of energy shells of the various organic molecules is very high (for example, 36 energy shells for deoxyribose), for each incident electron energy we would need to know the value of the cumulated ionisation probability of each shell to determine the secondary electron energy of emission. In other words, we would need to use large cross-section tables. Hence, in this work we are also introducing a novel sampling method to calculate the transferred secondary electron energy by means of an analytical sampling technique instead of applying the interpolation method from the differential ionisation cross section tables currently used in Geant4-DNA.

II. Materials and Methods:

a) Implementation of the physics model classes

Three new interaction model classes for elastic scattering, excitation and ionisation of electrons were implemented as Geant4-DNA physics models inherited from the G4VEmModel class [10]. Each model class tracks electrons in seven different materials (adenine, thymine, cytosine, guanine, deoxyribose, phosphoric acid, and liquid water) based on their total electron interaction cross sections. The energy range of incident electrons goes from 11 eV to 1 MeV for all materials, except for liquid water, which remains in the 11 eV - 256 keV energy range as in the previous implementation [21]. The total and differential cross section data tables for adenine, thymine, cytosine and guanine were calculated in a previous work [20], while, for deoxyribose and phosphoric acid, the calculations will be described in the following sections. Interpolation between consecutive energy points in the cross-section data tables was applied and electrons were tracked down to 11 eV, where tracks are killed and their energies were deposited locally. The scattering angle is randomly sampled according to the elastic angular differential cross section tables. The transferred energy by

ionisation is randomly sampled according to the ionisation energy differential cross section tables. In addition, a new analytical sampling method introduced in the following section has also been implemented, which allows the sampling of the transferred energy values as an alternative to the interpolation method. CSDA range and electronic stopping power were calculated using the Geant4-DNA examples "range" and "spower" [12] to verify the model classes and were then compared to data reported in the literature. A comparison between the interpolation and sampling methods was also carried out.

b) Physics models and cross-sections

For each mentioned process, the calculations of the cross sections for deoxyribose and phosphoric acid were based on the same models that we used for the four nucleobases adenine, thymine, cytosine and guanine and that are detailed in the previous paper by Zein *et al.* [20] for the same energy range [11 eV – 1 MeV].

Elastic scattering

The angular differential cross section at a certain incident energy is calculated using the independent atom model (IAM). This model required the internuclear distances between the atoms of the examined molecule, the angular differential cross section of each atom and the complex scattering amplitudes (see equation 1 in paper [20]).

For atoms, the scattering amplitudes and the differential cross sections were obtained from the Elastic Scattering of Electrons and Positrons by neutral Atoms (ELSEPA) code developed by Salvat *et al.* [23].

The structures of the considered molecules were obtained through geometry optimizations at Hartree-Fock/cc-pVTZ level, which were performed using the quantum chemistry package *Gaussian09* [24].

Ionisation

This process required the energy differential cross section for each molecular orbital and the corresponding integrated ionisation cross section over the ejected energy range in order to know which shell was concerned by this process and what was the energy transferred to the ejected electron. To this purpose, the Relativistic Binary Encounter Bethe Vriens (RBEBV) model was used [25]. The analytical forms (equations 2 and 4 in Zein *et al.* [20]) only depend on three parameters, which are representative of each molecular orbital and are determined from the molecular electronic structure. To accomplish this task, the molecular orbitals of each molecule were obtained through *ab initio* quantum chemistry calculations at restricted Hartree-Fock/cc-pVTZ level on the above-mentioned optimized molecular geometries using the GAMESS-UK software [26], as already done for the four DNA nucleobases in the previous paper by Zein *et al.* [20].

For deoxyribose, there are 36 molecular orbitals including 9 inner shells, while, for phosphoric acid, we have 25 molecular orbitals with 9 inner shells. The energy threshold varies from 11.24 eV to 559.77 eV for deoxyribose and from 13.00 eV to 2179.56 eV for phosphoric acid.

Table 1. Ionisation and excitation outer shell binding energy:

Binding energy (eV)	Water	Adenine	Cytosine	Guanine	Thymine	Deoxyribose	Phosphoric acid
Ionisation	10.79	8.51	9.32	8.23	9.64	11.24	13.00
Excitation	8.17	8.51	9.32	8.23	9.64	11.24	13.00

Excitation

The total excitation cross section was linked to the total ionisation cross section and to the ratio of the total excitation over ionisation cross section in water at a given incident energy, as it was proposed in the initial version of the CPA100 code [6].

With the assumption that only electronic levels lower than 20 eV can be excited, we considered 17 excitation levels for deoxyribose and 9 for phosphoric acid. We assumed that each level had the same probability to be chosen.

c) Sampling Method

Following the Relativistic Binary Encounter Bethe Vriens (RBEBV) model for each molecular orbital from the threshold to 1 MeV, the relativistic energy differential cross section written in the reduced form is (equation 2 in paper Zein *et al.* [20])

$$\frac{d\sigma}{dw} = \frac{4\pi a_0^2 \alpha^4 N}{(\beta_t^2 + \beta_u^2 + \beta_b^2) 2b'} \cdot \left[-\frac{\phi}{t+1} \cdot \left(\frac{1}{w+1} + \frac{1}{t-w} \right) \cdot \frac{1+2t'}{(1+t'/2)^2} + \frac{1}{(w+1)^2} + \frac{1}{(t-w)^2} + \frac{b'^2}{(1+t'/2)^2} + \left(Ln\left(\frac{\beta_t^2}{1-\beta_t^2} \right) - \beta_t^2 - Ln(2b') \right) . \left(\frac{1}{(w+1)^3} + \frac{1}{(t-w)^3} \right) \right] \quad (1)$$

With $w = \frac{W}{B}$

$\beta_t^2 = 1 - \frac{1}{(1+t')^2}$ and $t' = \frac{T}{mc^2}$ and $t = \frac{T}{B}$

$\beta_u^2 = 1 - \frac{1}{(1+u')^2}$ and $u' = \frac{U}{mc^2}$ and $u = \frac{U}{B}$

$\beta_b^2 = 1 - \frac{1}{(1+b')^2}$ and $b' = \frac{B}{mc^2}$

where α, m and c are the fine structure constant, the electron mass and the speed of light in vacuum, respectively.

T is the incident electron kinetic energy and W is the ejected electron kinetic energy. B (i.e., the bound electron binding energy), U (i.e., the bound electron kinetic energy), and N (i.e., the occupation number of the subshell to be ionized) are the three parameters representative of the molecular shell.

The relativistic form of the Vriens function ϕ is written as $\phi = \cos\left[\sqrt{\frac{\alpha^2}{(\beta_t^2+\beta_b^2)}}\,Ln\left(\frac{\beta_t^2}{\beta_b^2}\right)\right]$

To sample the reduced kinetic energy of the secondary electron w, the composition sampling method already used for the non-relativistic BEB version in liquid water (Bordage *et al.* [21]) was expanded and adapted for the DNA constituents. The equation must be written as the sum of positive functions of w, denoted $k_i(w)$:

$$\frac{d\sigma}{dw} = k_1(w) + k_2(w) + k_3(w) \tag{2}$$

The functions k_i can be decomposed as the product of three terms (A_i, h_i and g_i):

$$k_i(w) = A_i \cdot h_i(w) \cdot g_i(w) \tag{3}$$

which satisfy the following constraints

$$G_i = \int_0^{\frac{t-1}{2}} g_i(w)\,\mathrm{d}w = 1$$
$$\text{and } \forall w: \begin{cases} 0 \le h_i(w) \le 1 \\ g_i(w) \ge 0 \\ \exists\, G_i, G_i{}^{-1} \\ A_i \ge 0 \end{cases} \tag{4}$$

In order to respect these constraints, the k_i functions (eq 3) are written as

$$k_1(w) = \frac{4\pi a_0^2 \alpha^4 N}{(\beta_t^2+\beta_u^2+\beta_b^2)2b'} \cdot \left(\frac{1}{(w+1)^2} - \frac{\phi D}{(t+1)(w+1)} - \frac{\phi D}{2(t+1)(t-w)} + F\right)$$

$$k_2(w) = \frac{4\pi a_0^2 \alpha^4 N}{(\beta_t^2+\beta_u^2+\beta_b^2)2b'} \cdot \left(\frac{1}{(t-w)^2} - \frac{\phi D}{2(t+1)(t-w)}\right)$$

$$k_3(w) = \frac{4\pi a_0^2 \alpha^4 N}{(\beta_t^2+\beta_u^2+\beta_b^2)2b'} \cdot \frac{1}{(w+1)^3} \cdot \left(1 + \left(\frac{w+1}{t-w}\right)^3\right) \cdot \left(Ln\left(\frac{\beta_t^2}{1-\beta_t^2}\right) - \beta_t^2 - Ln(2b')\right)$$

where $D = \frac{1+2t\prime}{(1+t\prime/2)^2}$ and $F = \frac{b\prime^2}{(1+t\prime/2)^2}$

Each term of equation 3, fulfilling the constraints expressed through equation 4, can be decomposed as follows:

For the first function (k_1), we have:

$$A_1 = \frac{4\pi a_0^2 \alpha^4 N}{(\beta_t^2 + \beta_u^2 + \beta_b^2) 2b'} \cdot \frac{t-1}{t+1} \cdot \frac{(1+F)2t(t+1) - \phi D(2t+1)}{2t(t+1)}$$

$$g_1(w) = \frac{t+1}{t-1} \frac{1}{(w+1)^2};$$

$$h_1(w) = \left[1 - \frac{\phi D(w+1)}{(t+1)} \left(1 + \frac{(w+1)}{2(t-w)}\right) + F(w+1)^2\right] \cdot \frac{2t(t+1)}{(1+F)2t(t+1) - \phi D(2t+1)}$$

For the second one (k_2):

$$A_2 = \frac{4\pi a_0^2 \alpha^4 N}{(\beta_t^2 + \beta_u^2 + \beta_b^2) 2b'} \cdot \frac{t-1}{t(t+1)} \frac{4 - \phi D}{4}$$

$$g_2(w) = \frac{t(t+1)}{t-1} \frac{1}{(t-w)^2};$$

$$h_2(w) = \left(1 - \frac{\phi D(t-w)}{2(t+1)}\right) \cdot \frac{4}{4 - \phi D}$$

and for the third one (k_3):

$$A_3 = \frac{4\pi a_0^2 \alpha^4 N}{(\beta_t^2 + \beta_u^2 + \beta_b^2) 2b'} \cdot \left(Ln\left(\frac{\beta_t^2}{1-\beta_t^2}\right) - \beta_t^2 - Ln(2b')\right) \frac{(t+1)^2 - 4}{(t+1)^2}$$

$$g_3(w) = \frac{2(t+1)^2}{(t+1)^2 - 4} \cdot \frac{1}{(w+1)^3}$$

$$h_3(w) = \frac{1}{2}\left(1 + \left(\frac{w+1}{t-w}\right)^3\right)$$

The $g_i(w)$ functions were defined in order for the cumulative distribution function G_i to exist and to have an inverse function.

Furthermore, as it was developed in the appendix of the paper by Bordage *et al.* [21], two steps are required for the sampling:

a- The generation of the first random number, R_1, to select which k_i function should be sampled, such as:

$$\sum_{i=1}^{k-1} A_i \leq R_1 \sum_{i=1}^{3} A_i \leq \sum_{i=1}^{k} A_i$$

b- Once the k_i function is chosen, the generation of a second random number R_2 to generate the energy loss w_x with respect to the probability density g_i, so that $\int_0^{w_x} g_i(w)\,\mathrm{d}w = R_2$ and w_x is rejected if $R_3 > h_k(w_x)$

III. Results:

a) Total Cross Sections of deoxyribose and phosphoric acid:

Figure 1 (a) shows the calculated total cross sections as a function of the electron incident energy for the three processes (elastic scattering, excitation and ionisation) and for the two studied materials (deoxyribose and phosphoric acid). For comparison, the curves for adenine [20] and liquid water-option6 [21] implemented in Geant4-DNA are also plotted. The results for adenine and deoxyribose are very close and are higher than those for phosphoric acid for all incident energies.

As an example, Figure 1 (b) shows the variation of the differential elastic cross section as a function of the scattering angle at an incident energy of 100 eV for phosphoric acid and deoxyribose. The results are compared with differential cross section in adenine and water, as well as with the only published calculations at this energy by Mozejko and Sanche [27].

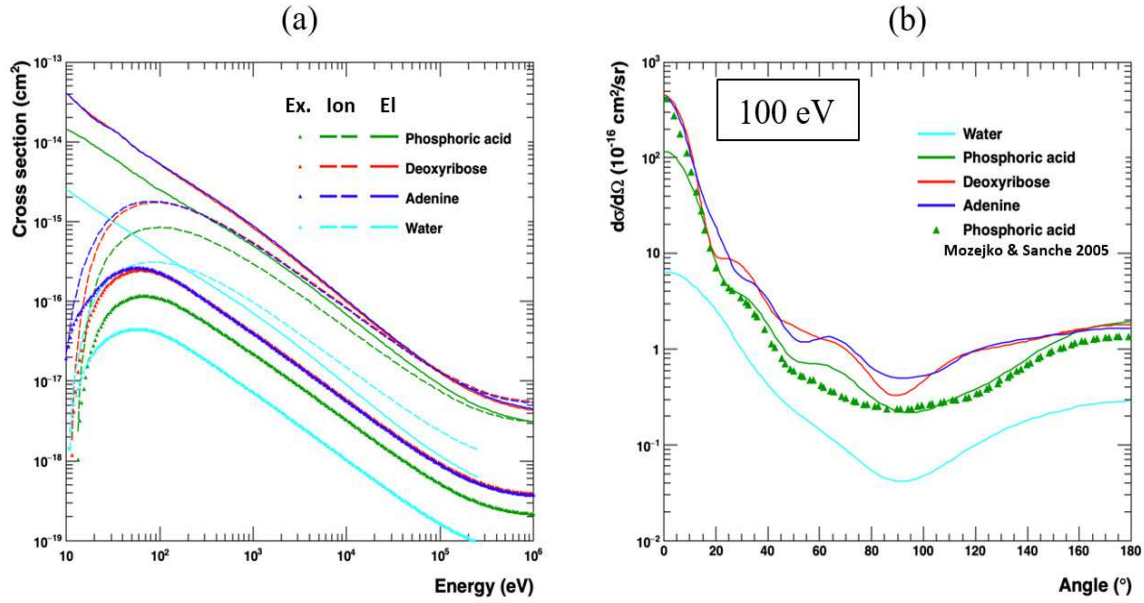

Figure 1. (a) Total cross sections for elastic scattering (El), excitation (Ex) and ionisation (Ion) for deoxyribose and phosphoric acid compared to adenine [20] and water-option6 [21].
(b) Differential elastic cross section for incident energy of 100 eV for deoxyribose and phosphoric acid, compared to adenine [20] and liquid water-option6 [21] and the published calculated data by Mozejko and Sanche [27] for phosphoric acid.

Figure 2 (a) shows the total elastic cross sections of deoxyribose and phosphoric acid as a function of the incident energy. The comparison with the work of Mozejko on phosphoric acid [27] is also shown. In Figure 2 (b) the total ionisation cross sections of deoxyribose and phosphoric acid are depicted and compared with published data reported in the literature [27-29]. There are no other theoretical or experimental data for cross sections of phosphoric acid and deoxyribose available for comparison.

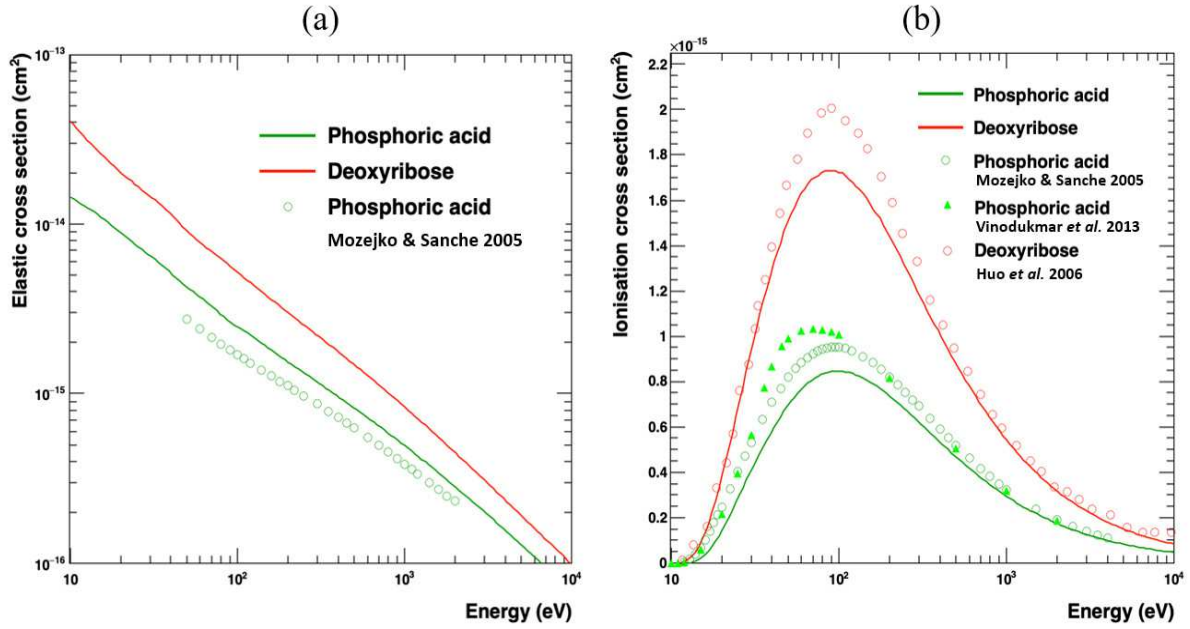

Figure 2. Comparison of the present cross sections (continuous lines) with calculations from the literature (symbols) (a) for elastic scattering in phosphoric acid done by Mozejko and Sanche [27], and (b) for the total ionisation cross section in deoxyribose done by Huo et al. [28] and phosphoric acid done by Mozejko and Sanche [27] and by Vinodukmar et al. [29].

b) Range

Figure 3 shows the range in all materials as calculated using the updated version of the "option 6" physics models over the 11 eV – 1 MeV energy range (11 eV – 256 keV for liquid water). The comparison with calculations reported in the literature shows a good agreement for energies higher than 1 keV, while for the comparison with liquid water we can observe some differences at low energies (< 1keV). Figures 3 (e) and (f) show the range in deoxyribose and phosphoric acid calculated with a low energy cut of 14 eV, below which the energy was deposited locally. Since the excitation and ionisation energy levels of deoxyribose and phosphoric acid are higher than the low energy limit 11 eV, the 14 eV cut was tested as the first energy above the inelastic outer shell binding energies (see Table 1). This indicates that the range is affected by elastic scattering at low sub-inelastic energies of deoxyribose and phosphoric acid (Table 1).

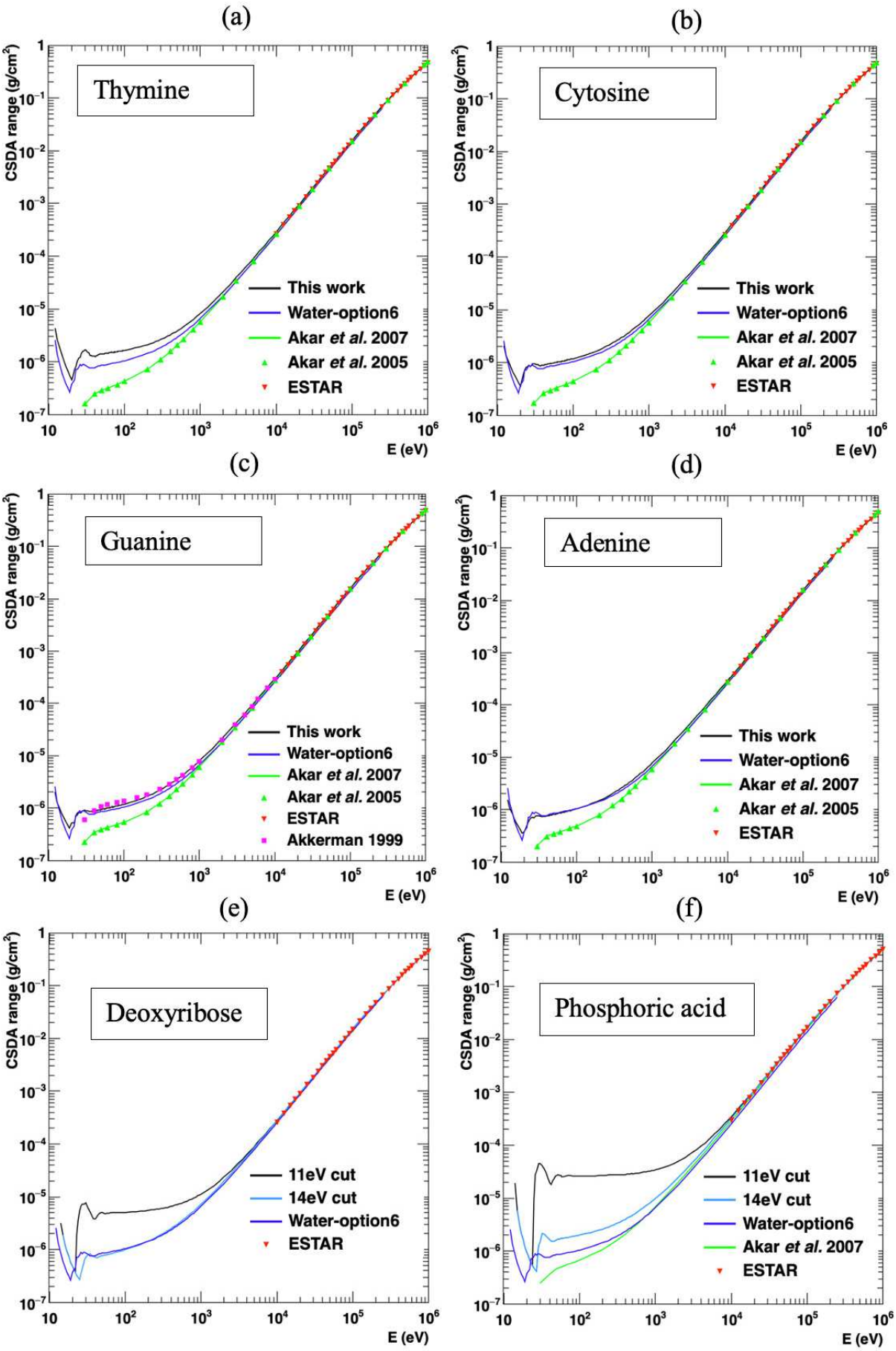
(a)
Thymine
This work
Water-option6
Akar et al. 2007
Akar et al. 2005
ESTAR
(b)
Cytosine
This work
Water-option6
Akar et al. 2007
Akar et al. 2005
ESTAR
(c)
Guanine
This work
Water-option6
Akar et al. 2007
Akar et al. 2005
ESTAR
Akkerman 1999
(d)
Adenine
This work
Water-option6
Akar et al. 2007
Akar et al. 2005
ESTAR
(e)
Deoxyribose
11eV cut
14eV cut
Water-option6
ESTAR
(f)
Phosphoric acid
11eV cut
14eV cut
Water-option6
Akar et al. 2007
ESTAR
CSDA range (g/cm²)
E (eV)

337

Figure 3. CSDA range calculated for (a) thymine, (b) cytosine, (c) guanine, (d) adenine, (e) deoxyribose and (f) phosphoric acid in Geant4-DNA and compared to water "option 6" [21], data from the literature (Akar et al. 2005 [30], Akar et al. 2007 [31], Akkerman 1999 [32]) and the ESTAR database [33]. Panels (a), (b), (c), and (d) show the ranges calculated with 11 eV cut (black curves) which is the lowest value in the implemented energy range. Panels (e) and (f) show the effect of the energy cut-off on the range calculation with 11 eV cut (in black) set at the low energy limit and 14 eV cut (in light blue) just above the first ionisation level of phosphoric acid.

a) Stopping Power

Figure 4 shows the electronic stopping power calculation in deoxyribose and phosphoric acid in comparison with the work of Akar 2007 *et al.* [31], which is currently the only available calculation in the literature for phosphoric acid. We also compared with calculations from the ESTAR database [33], which depend on the densities and the chemical formula of the deoxyribose ($C_5H_{10}O_4$) and phosphoric acid (H_3PO_4). Densities and chemical formulas for each material are given in Table 2.

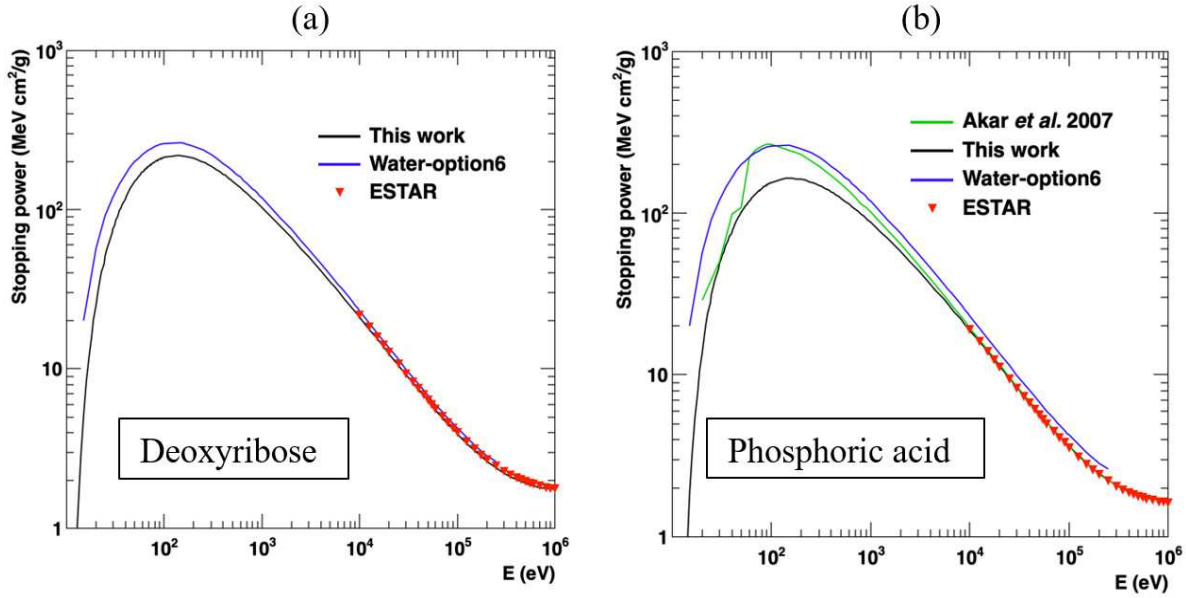

Figure 4. Electronic stopping power calculated for (a) deoxyribose and (b) phosphoric acid in Geant4-DNA and compared to water-option 6 [21], data from the literature calculated by Akar et al. [31] and the ESTAR database [33].

c) Comparison of interpolation and sampling methods:

Figure 5 shows the range and electronic stopping power of electrons in phosphoric acid calculated using the method based on the interpolation of tabulated cross section data and the sampling method. The same test was performed for the other materials and the difference between the sampling and interpolation methods was less than 1.5% difference in stopping power and less than 4% difference in range for all the six examined materials.

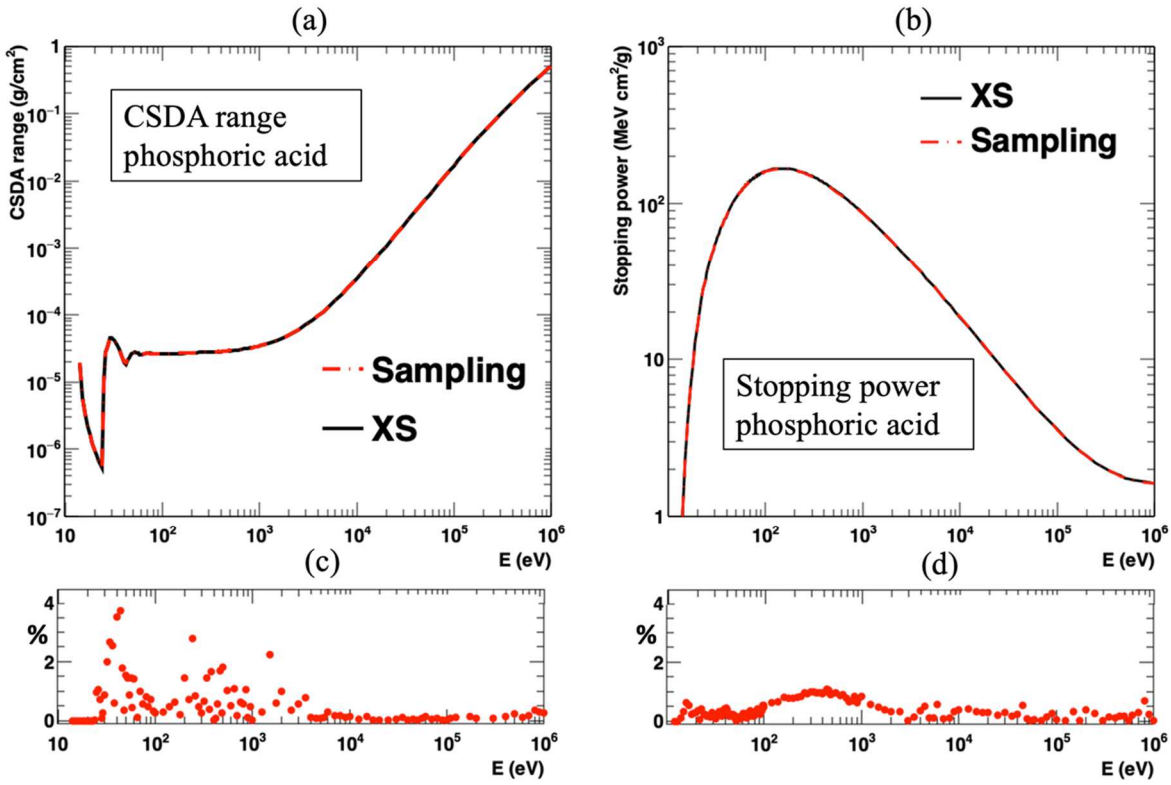

Figure 5. (a) CSDA range and (b) stopping power of phosphoric acid calculated with sampling and interpolation (XS) methods of ionisation differential cross sections. Panels (c) and (d) show the absolute percentage difference of range and stopping power by the sampling method relative to the interpolation method.

d) Interaction type ratio

In Figure 6 (a) the CSDA range of electrons in all 7 materials with 11 eV cutoff is shown. Phosphoric acid and deoxyribose have larger ranges at energies lower than 10 keV compared to the other materials due to their high contribution of elastic scattering in the sub-inelastic range. The CSDA range shows direct dependence on the density of the materials for energies above 10 keV. Figure 6 (b) shows the electronic stopping power in all the materials under study. Above 200 eV, the stopping power is directly proportional to the density of the material while for the lower energies the interaction cross-sections influence the stopping power. In Figure 6 (c) the ratio of the three interactions per electron event as a function of energy is calculated. Only the first interaction was registered per incident electron event, and the total number of interaction types was calculated and then normalized to the total number of events. 10^6 events were tested per material. This calculation reflects the interaction type probability to occur per electron energy. The cross-section type ratio to the total cross section by all the three interactions in deoxyribose is shown in Figure 6 (d) in comparison to the ratio between the number of interaction types and the total number of interactions per incident electron. As expected, the calculated ratio of interactions from the simulations agrees well with the ratio of cross sections for all three types of interactions. The same results were found for all the materials under investigation (for the sake of simplicity, only deoxyribose is shown here), which assures the correct implementation of the interaction models in the simulation.

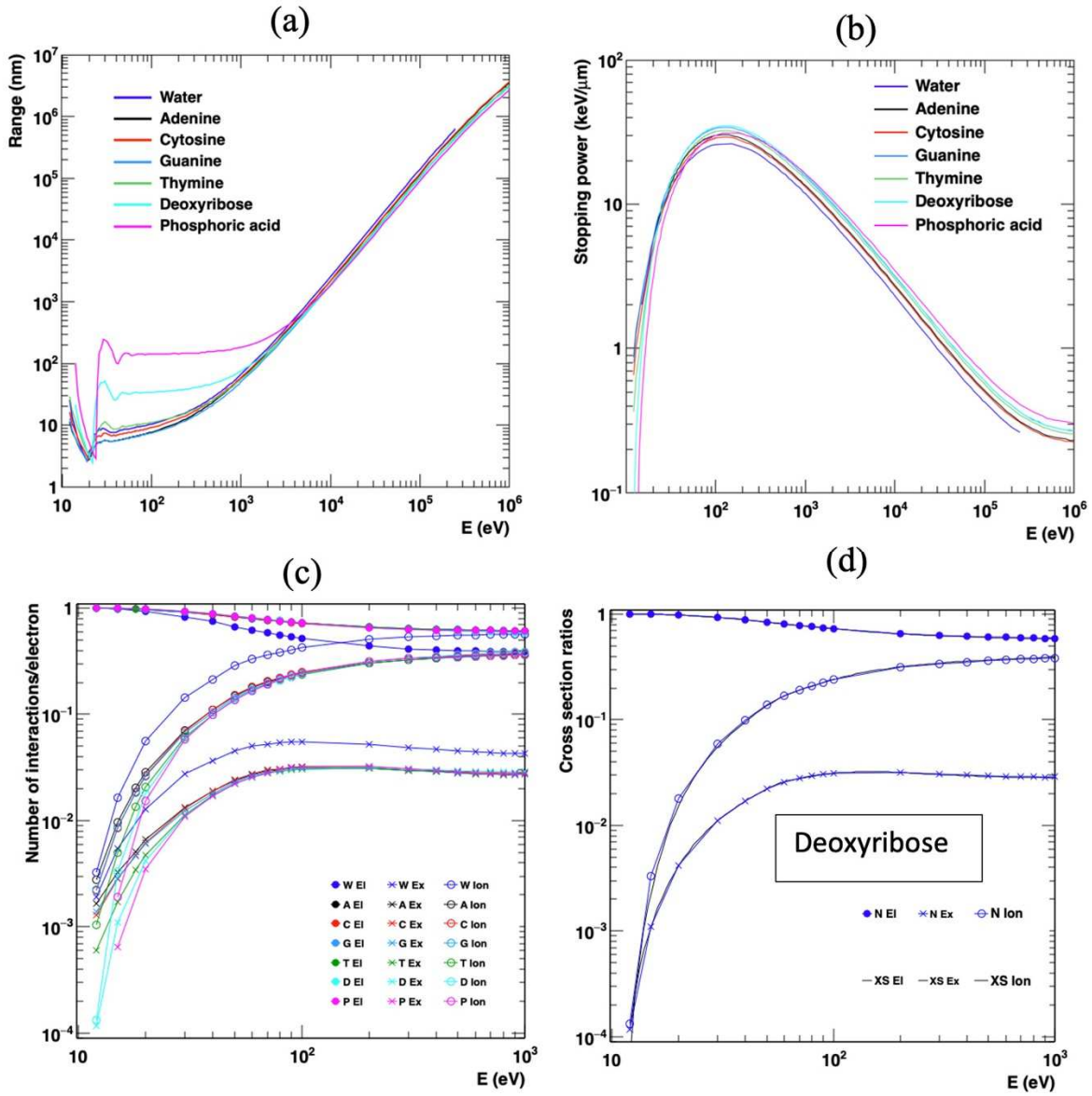

Figure 6. (a) CSDA range of the 7 different materials with 11 eV low energy cutoff. (b) Electronic stopping power of the 7 different materials. (c) Ratio of the number of interactions per incident electron in the 7 different materials. Legend symbols: W (Water), A (adenine), C (cytosine), G (guanine), T (thymine), D (deoxyribose), P (phosphoric acid), El (elastic scattering), Ex (excitation), Ion (ionisation). (d) Ratio of the number of interactions per incident electron in comparison with the cross-section ratios of deoxyribose. Legend symbols: N (number of interactions/incident electron) and XS (cross section type ratio to the total cross section of all 3 interactions).

Table 2. Chemical formulas and densities of the materials [19, 34, 35]

	Water	Adenine	Cytosine	Guanine	Thymine	Deoxyribose	Phosphoric acid
Formula	H_2O	$C_5H_5N_5$	$C_4H_5N_3O$	$C_5H_5N_5O$	$C_5H_6N_2O_2$	$C_5H_{10}O_4$	H_3PO_4
Density	1	1.35	1.3	1.58	1.48	1.5	1.87

(g/cm^3)							

IV. Discussion:

Monte Carlo track structure codes provide good tools for estimating DNA damages; however, the so far performed Monte Carlo studies on DNA damage considered liquid water as a surrogate of the biological medium and this led to underestimate the damage rate of the DNA molecule itself [5, 17, 18]. This limitation is what motivated our previous work, where we introduced new calculations of electron interaction cross sections in the four DNA bases for elastic scattering, excitation and ionization [20]. These cross sections were used in the implementation of new physics models of electrons for the purpose of extending the Geant4-DNA toolkit tracking capabilities in the DNA material. In this work, the electron interaction cross sections in the deoxyribose sugar and the phosphoric acid are calculated to complete the physics models in all DNA components.

The total cross sections of the three electron interactions, elastic scattering, excitation and ionization, with all DNA material are higher than those of liquid water, as shown in our previous work [20] and in Figure 1(a). Cross sections of deoxyribose are very close to those of adenine; however, they are higher than those of phosphoric acid for all incident energies. In addition, the densities of the DNA components are higher than liquid water as shown in Table 2. Therefore, the rate of particle with DNA interaction is expected to be higher than the one with water interaction, which emphasizes the inaccuracy of substituting water for DNA at the sub-cellular scale in Monte Carlo simulation studies.

The limited data available in the literature for this type of calculations makes it difficult to perform thorough comparisons, specifically for the deoxyribose and the phosphate. The only available elastic scattering cross section data in the literature are limited to theoretical values for phosphoric acid. Differential and integrated cross sections are calculated at energies between 50 eV and 2 keV by Mozejko and Sanche [27]. The present integrated elastic cross sections values are higher than those of reference [27] (Figure 2 (a)). Comparison of elastic differential cross section for phosphoric acid at 100 eV shows an overall good agreement with the calculations of Mozejko and Sanche for most scattering angles, with lower values at very small scattering angles (< 20°) (Figure 1 (b)). The data between 0 and 25 eV (Winstead et McKoy [36], Tonzani and Greene [37]) are not included.

For ionisation, we can compare only the total cross section (sum of the contribution of each orbital) with the only available theoretical results of Huo *et al.* [28] based on BEB method for deoxyribose, and for phosphoric acid with two different calculations (Mozejko and Sanche [27] and Vinodkumar *et al.* [29]). The results are in a relatively good agreement except in the energy range lower than 100 eV for phosphoric acid. Moreover, the present data are lower than those resulting from other calculations (Figure 2 (b)).

During the extension of these models previously implemented for the four DNA nucleobases [20], a bug was identified on the sampling of excitation, which affects only the range results at very low energy but neither the stopping power nor the inelastic mean free path. Therefore, after fixing the bug in the code, in this manuscript we decided to include the

updated range figures for the four DNA nucleobases adenine, thymine, guanine and cytosine (see panels a, b, c and d in Figure 3).

At high energy, a good agreement in range is observed with the published data, with a deviation at low energy (<1 keV) for all four nucleobases. The range is different than the one obtained from the liquid water calculation through Geant4-DNA using the same lower cutoff energy of 11 eV for all materials and the same physics models of the "option6" Geant4-DNA constructor. The new update affects the range curve at energies lower than 1 keV, where the CSDA range of the four nucleobases are closer to that of liquid water. Note that the range curves are normalized to the density of the material. At very low energy (<100 eV), thymine shows higher CSDA range values than adenine, cytosine and guanine, (see Figure 6 (a)) which is due to the lower inelastic cross sections of thymine compared to adenine, cytosine and guanine for energies less than 30 eV. This results in an elevated number of elastic scattering interactions at low energies. Because of the higher occurrence probability of elastic scattering, elastic scattering becomes highly dominant compared to excitation and ionisation, thus leading to longer electron tracks and, consequently, to a higher range (Figure 3 (a)). This can also be seen in Figure 6 (c), where excitation and ionisation probabilities of thymine are lower than adenine, cytosine and guanine for energies lower than 30 eV, consequently leading to a greater dominance of elastic scattering.

Deoxyribose and phosphoric acid have the outermost binding energy values, in particular higher than the tracking energy cutoff of 11 eV (11.24 eV for deoxyribose and 13 eV for phosphoric acid, Table 1). Therefore, when an electron reaches energies below the binding energy threshold, only elastic scattering takes place and leads to long electron tracks without significant energy loss. This significantly affects the CSDA range of phosphoric acid and, to a lesser extent, the CSDA range of deoxyribose for low energies (< 1 keV), as shown in Figures 3 (e) and (f) also Figure 6 (a). Similar to thymine, deoxyribose and phosphoric acid have lower inelastic probabilities at energies lower than 30 eV (Figure 6 (c)), which also contributes to the high CSDA range at low energies. When calculating the range with a 14 eV energy cutoff for deoxyribose and phosphoric acid, which is higher than the lowest binding energy of phosphoric acid, the range dramatically decreases and becomes closer to water at very low energies due to the higher contribution of the inelastic processes and the limited effect of elastic scattering. Because of the high binding energies of the DNA backbone components, one should pay attention to the energy cutoff used for simulations, which might affect the results.

Stopping power calculations of both deoxyribose and phosphoric acid show a good agreement with the very scarce data from the literature, and an obvious difference from the liquid water calculations of Geant4-DNA is observed over the entire energy range (Figure 4). For low energies, the phosphoric acid has a lower collision stopping power than the one resulting from the calculations performed by Akar *et al*. [31] . The peak in this work is reached at 120 eV compared to 80 eV in the work by Akar and coworkers.

The sampling method introduced in this work allows efficient calculations of the secondary transferred energy after ionisation interaction. The conventional way through which Geant4-DNA calculates the secondary electron kinetic energy currently uses an interpolation method that samples the energy from tabulated data and applies an interpolation function that estimates the energy from two consecutive values corresponding to an ionisation shell. This normally requires a differential cross sections table file providing the incident energy intervals as well as the corresponding cumulative distribution of energy loss for each

ionisation shell. Since the incident energy range is extended up to 1 MeV and the biological molecules have a high number of ionisation shells (> 29) compared to liquid water (5 ionisation shells), the required data files become large to handle, build and distribute within the Geant4 toolkit. Therefore, the sampling method provides a convenient solution without affecting the outcome of the simulation results. In addition, calculating the transferred energy directly within the code represents a more accurate method than interpolation between two consecutive energy values, which may introduce some variation if the difference between the two energies is not sufficiently small. The differences between the sampling and the interpolation methods showed a maximum of 4% for CSDA range calculations and less than 2% for collision stopping power computations for all materials (Figures 5 (c) and (d)). However, the sampling method does not have any advantage over the interpolation concerning the computational cost. A similar method based on the binary encounter Bethe model was already introduced and is currently available for liquid water [21]. The sampling routine can also be applied with materials for which the relativistic binary encounter Bethe relativistic energy differential cross sections are used (equation 1). For the moment, it could be used directly not only for the four DNA nucleobases [20], deoxyribose and phosphoric acid but also for gold [38]. Another advantage of this work is that the here-presented approach could be exploited in future applications of Geant4-DNA damage models calculation, where the physics constructor "option6" could be used in combination with the detailed DNA geometry introduced by Lampe, especially because we are using the same architecture and chemical composition of the DNA constituents [39, 40].

V. Conclusion:

In this study, an update of the Geant4-DNA physics constructor "option 6" was described. This update includes a full set of electron interaction cross-sections for elastic scattering, electronic excitation and ionisation for the different components of the DNA molecule, in addition to those already available for liquid water. The model has been tested considering CSDA range and stopping power of electrons for the various DNA components, where we observed a good agreement with data available in the literature. In addition, a novel sampling method for calculating the secondary ionisation electrons kinetic energy was introduced, which will reduce the total memory allocated for the ionisation differential cross-section tables.

This work represents a stepping stone for particle interaction simulations with organic materials not limited to DNA only. The methods and architecture of the physics models can be translated to other molecules, such as amino acids that make up proteins. In combination with detailed geometry, more realistic simulations at the subcellular scale could be achieved, which would lead to better understanding of radiation effects on biological material. The physics models could also be adapted and expanded for the cross-section calculation of other particles, such as protons. The sampling method introduced could be used as an efficient alternative for interpolation methods in future releases of Geant4-DNA. All in all, the complete package of electron interactions in the DNA constituents provides a novel tool for a new generation of Monte Carlo simulations.

Acknowledgements:

The authors would like to thank Dr. Dousatsu Sakata for his valuable advice.

References:

1. Borges, H.L., R. Linden, and J.Y.J. Wang, *DNA damage-induced cell death: lessons from the central nervous system.* Cell Research, 2008. **18**(1): p. 17-26.
2. Chatterjee, N. and G.C. Walker, *Mechanisms of DNA damage, repair, and mutagenesis.* Environmental Molecular Mutagenesis, 2017. **58**(5): p. 235-263.
3. El Naqa, I., P. Pater, and J. Seuntjens, *Monte Carlo role in radiobiological modelling of radiotherapy outcomes.* Physics in Medicine and Biology, 2012. **57**(11): p. R75-97.
4. Nikjoo, H., et al., *Track-structure codes in radiation research.* Radiation Measurements, 2006. **41**(9): p. 1052-1074.
5. Friedland, W., et al., *Comprehensive track-structure based evaluation of DNA damage by light ions from radiotherapy-relevant energies down to stopping.* Scientific Reports, 2017. **7**: p. 45161.
6. Terrissol, M. and A. Beaudre, *Simulation of space and time evolution of radiolytic species induced by electrons in water.* Radiation Protection Dosimetry, 1990. **31**(1-4): p. 175-177.
7. Edel, S., *Modélisation du transport des photons et des électrons dans l'ADN plasmide*. 2006, PhD Thesis, Université Toulouse III-Paul Sabatier, Toulouse, France.
8. Peudon, A., *Prise en compte de la structure moléculaire pour la modélisation des dommages biologiques radio-induits*. 2007, PhD Thesis, Université Toulouse III-Paul Sabatier, Toulouse, France.
9. Bernal, M.A., et al., *Track structure modeling in liquid water: A review of the Geant4-DNA very low energy extension of the Geant4 Monte Carlo simulation toolkit.* Physica Medica: European Journal of Medical Physics, 2015. **31**(8): p. 861-874.
10. Incerti, S., et al., *The Geant4-DNA Project.* International Journal of Modeling, Simulation, and Scientific Computing, 2010. **01**(02): p. 157-178.
11. Incerti, S., et al., *Comparison of GEANT4 very low energy cross section models with experimental data in water.* Medical Physics, 2010. **37**(9): p. 4692-4708.
12. Incerti, S., et al., *Geant4-DNA example applications for track structure simulations in liquid water: A report from the Geant4-DNA Project.* Medical Physics, 2018. **45**(8): p. e722-e739.
13. Agostinelli, S., et al., *GEANT4—a simulation toolkit.* Nuclear Instruments and Methods in Physics Research A, 2003. **506**(3): p. 250-303.
14. Allison, J., et al., *Geant4 developments and applications.* IEEE Transactions on Nuclear Science, 2006. **53**(1): p. 270-278.
15. Allison, J., et al., *Recent developments in Geant4.* Nuclear Instruments and Methods in Physics Research A, 2016. **835**: p. 186-225.
16. Karamitros, M., et al., *Modeling Radiation Chemistry in Geant4 Toolkit.* Nuclear Science and Technology, 2011. **2**: p. 505 - 508.
17. Friedland, W., et al., *Simulation of DNA damage after proton irradiation.* Radiation Research, 2003. **159**(3): p. 401-10.
18. Francis, Z., C. Villagrasa, and I. Clairand, *Simulation of DNA damage clustering after proton irradiation using an adapted DBSCAN algorithm.* Computer Methods and Programs in Biomedicine, 2011. **101**(3): p. 265-270.
19. Tan, Z., et al., *Proton stopping power in a group of bioorganic compounds over the energy range of 0.05–10MeV.* Nuclear Instruments and Methods in Physics Research Section B: Beam Interactions with Materials and Atoms, 2006. **248**(1): p. 1-6.

20. Zein, S.A., et al., *Electron transport in DNA bases: An extension of the Geant4-DNA Monte Carlo toolkit.* Nuclear Instruments and Methods in Physics Research Section B: Beam Interactions with Materials and Atoms, 2021. **488**: p. 70-82.
21. Bordage, M.-C., et al., *Implementation of new physics models for low energy electrons in liquid water in Geant4-DNA.* Physica Medica, 2016. **32**(12): p. 1833-1840.
22. Peudon, A., S. Edel, and M. Terrissol, *Molecular basic data calculation for radiation transport in chromatin.* Radiation protection dosimetry, 2006. **122**(1-4): p. 128-135.
23. Salvat, F., A. Jablonski, and C.J. Powell, *ELSEPA—Dirac partial-wave calculation of elastic scattering of electrons and positrons by atoms, positive ions and molecules.* Computer Physics Communications, 2005. **165**(2): p. 157-190.
24. Frisch, M.J.T., G. W.; Schlegel, H. B.; Scuseria, G. E.; Robb, M. A.; Cheeseman, J. R.; Scalmani, G.; Barone, V.; Mennucci, B.; Petersson, G. A.; Nakatsuji, H.; Caricato, M.; Li, X.; Hratchian, H. P.; Izmaylov, A. F.; Bloino, J.; Zheng, G.; Sonnenberg, J. L.; Hada, M.; Ehara, M.; Toyota, K.; Fukuda, R.; Hasegawa, J.; Ishida, M.; Nakajima, T.; Honda, Y.; Kitao, O.; Nakai, H.; Vreven, T.; Montgomery, J. A., Jr.; Peralta, J. E.; Ogliaro, F.; Bearpark, M.; Heyd, J. J.; Brothers, E.; Kudin, K. N.; Staroverov, V. N.; Kobayashi, R.; Normand, J.; Raghavachari, K.; Rendell, A.; Burant, J. C.; Iyengar, S. S.; Tomasi, J.; Cossi, M.; Rega, N.; Millam, J. M.; Klene, M.; Knox, J. E.; Cross, J. B.; Bakken, V.; Adamo, C.; Jaramillo, J.; Gomperts, R.; Stratmann, R. E.; Yazyev, O.; Austin, A. J.; Cammi, R.; Pomelli, C.; Ochterski, J. W.; Martin, R. L.; Morokuma, K.; Zakrzewski, V. G.; Voth, G. A.; Salvador, P.; Dannenberg, J. J.; Dapprich, S.; Daniels, A. D.; Farkas, Ö.; Foresman, J. B.; Ortiz, J. V.; Cioslowski, J.; Fox, D. J., *Gaussian 09, Revision D.01*. 2009: Wallingford, CT, USA.
25. Guerra, M., et al., *Single differential electron impact ionization cross sections in the binary-encounter-Bethe approximation for the low binding energy regime.* Journal of Physics B: Atomic, Molecular and Optical Physics, 2015. **48**(18): p. 185202.
26. Guest, M.F., et al., *The GAMESS-UK electronic structure package: algorithms, developments and applications.* Molecular Physics, 2005. **103**(6-8): p. 719-747.
27. Możejko, P. and L. Sanche, *Cross sections for electron scattering from selected components of DNA and RNA.* Radiation Physics and Chemistry, 2005. **73**(2): p. 77-84.
28. Huo, W.M., C.E. Dateo, and G.D. Fletcher, *Molecular data for a biochemical model of DNA damage: Electron impact ionization and dissociative ionization cross sections of DNA bases and sugar-phosphate backbone.* Radiation Measurements, 2006. **41**(9-10): p. 1202-1208.
29. Vinodkumar, M., et al., *Electron impact total ionization cross sections for all the components of DNA and RNA molecule.* International Journal of Mass Spectrometry, 2013. **339-340**: p. 16-23.
30. Akar, A. and H. Gümüş, *Electron stopping power in biological compounds for low and intermediate energies with the generalized oscillator strength (GOS) model.* Radiation Physics and Chemistry, 2005. **73**(4): p. 196-203.
31. Akar, A., H. Gümüş, and N. Okumuşoğlu, *Total electron stopping powers and CSDA-ranges from 20 eV to 10 MeV electron energies for components of DNA and RNA.* Advances in Quantum Chemistry, 2007. **52**: p. 277-288.
32. Akkerman, A. and E. Akkerman, *Characteristics of electron inelastic interactions in organic compounds and water over the energy range 20–10000 eV.* Journal of Applied Physics, 1999. **86**(10): p. 5809-5816.

33. Berger, M.J., et al. *ESTAR, PSTAR, and ASTAR: Computer Programs for Calculating Stopping-Power and Range Tables for Electrons, Protons, and Helium Ions (version 1.2.3).* 2005; Available from: http://physics.nist.gov/Star
34. Egan, E.P. and B.B. Luff, *Measurements at 15°to 80° C. - Density of Aqueous Solutions of Phosphoric Acid.* Industrial & Engineering Chemistry, 1955. **47**(6): p. 1280-1281.
35. *ACD Labs Percepta Plateform - PhysChem Module*. Available from: https://www.acdlabs.com/products/percepta/index.php
36. Winstead, C. and V. McKoy, *Interaction of slow electrons with methyl phosphate esters.* International Journal of Mass Spectrometry, 2008. **277**(1-3): p. 279-283.
37. Tonzani, S. and C.H. Greene, *Radiation damage to DNA: Electron scattering from the backbone subunits.* The Journal of Chemical Physics, 2006. **125**(9): p. 094504.
38. Sakata, D., et al., *An implementation of discrete electron transport models for gold in the Geant4 simulation toolkit.* Journal of Applied Physics, 2016. **120**(24): p. 244901.
39. Lampe, N., et al., *Mechanistic DNA damage simulations in Geant4-DNA part 1: A parameter study in a simplified geometry.* Physica Medica, 2018. **48**: p. 135-145.
40. Lampe, N., *The long term impact of ionising radiation on living systems.* 2017, PhD Thesis, Université Clermont Auvergne, France.